

Optical 4x4 hitless silicon router for optical Networks-on-Chip (NoC)

Nicolás Sherwood-Droz^{1*}, Howard Wang², Long Chen¹, Benjamin G. Lee², Aleksandr Biberman², Keren Bergman², Michal Lipson¹

School of Electrical and Computer Engineering, Cornell University, Ithaca, N.Y. 14850

Department of Electrical Engineering, Columbia University, New York, N.Y. 10027

*Corresponding author: nrs35@cornell.edu

Abstract: We demonstrate here a spatially non-blocking optical 4x4 router with a footprint of 0.07 mm² for use in future integrated photonic interconnection networks. The device is dynamically switched using thermo-optically tuned silicon microring resonators with a wavelength shift to power ratio of 0.25nm/mW. The design can route four optical inputs to four outputs with individual bandwidths of up to 38.5 GHz. All tested configurations successfully routed a single-wavelength laser and provided a maximum extinction ratio larger than 20 dB.

©2008 Optical Society of America

OCIS codes: (060.4250) Fiber optics and optical communications: Networks; (130.4815) Integrated optics: Optical switching devices; (230.3990) Optical devices: Micro-optical devices.

References and links

1. A. Shacham, K. Bergman, and L. P. Carloni, "On the Design of a Photonic Network-on-Chip," in *Networks-on-Chip* (2007), pp. 53-64.
2. R. G. Beausoleil, P. J. Kuekes, G. S. Snider, W. Shih-Yuan, and R. S. Williams, "Nanoelectronic and Nanophotonic Interconnect," *Proc. IEEE* **96**, 230-247 (2008).
3. J. Lexau, X. Zheng, J. Bergey, A. V. Krishnamoorthy, R. Ho, R. Drost, and J. Cunningham, "CMOS Integration of Capacitive, Optical, and Electrical Interconnects," *International Interconnect Technology Conference, IEEE 2007*, 78-80 (2007).
4. M. Briere, B. Girodias, Y. Bouchebaba, G. Nicolescu, F. Mieyeville, F. Gaffiot, and I. O. Connor, "System level assessment of an optical NoC in an MPSoC platform," in *Proceedings of the conference on Design, automation and test in Europe* (EDA Consortium, Nice, France, 2007).
5. B. A. Small, B. G. Lee, K. Bergman, Q. Xu, and M. Lipson, "Multiple-wavelength integrated photonic networks based on microring resonator devices," *J. Opt. Netw.* **6**, 112-120 (2007).
6. F. Xia, M. Rooks, L. Sekaric, and Y. Vlasov, "Ultra-compact high order ring resonator filters using submicron silicon photonic wires for on-chip optical interconnects," *Opt. Express* **15**, 11934-11941 (2007).
7. S. T. Chu, B. E. Little, W. Pan, T. A. Kaneko, S. A. Sato, and Y. A. Kokubun, "An eight-channel add-drop filter using vertically coupled microring resonators over a cross grid," *Photonics Technology Letters, IEEE* **11**, 691-693 (1999).
8. B. E. Little, S. T. Chu, W. Pan, and Y. A. K. Y. Kokubun, "Microring resonator arrays for VLSI photonics," *Photon. Technol. Lett. IEEE* **12**, 323-325 (2000).
9. L. Zhang, M. Yang, Y. Jiang, E. Regentova, and E. Lu, "Generalized Wavelength Routed Optical Micronetwork in Network-on-Chip," *Proceedings of the 18 th IASTED International Conference on Parallel and Distributed Computing and Systems* (2006).
10. W. J. Dally, *Principles and Practices of Interconnection Networks* (Morgan Kaufmann, 2004).
11. A. Shacham, B. G. Lee, A. Biberman, K. Bergman, and L. P. Carloni, "Photonic NoC for DMA Communications in Chip Multiprocessors," in *15th Annual IEEE Symposium on High-Performance Interconnects (HOTI 2007)*(2007), pp. 29-38.
12. H. Wang, M. Petracca, A. Biberman, B. G. Lee, L. P. Carloni, and K. Bergman, "Nanophotonic Optical Interconnection Network Architecture for On-Chip and Off-Chip Communications," in *Optical Fiber communication/National Fiber Optic Engineers Conference*(2008), pp. 1-3.
13. C. R. Pollock, and M. Lipson, *Integrated Photonics* (Kluwer Academic Publishers, 2003).
14. S. N. Magdalena, L. Tao, W. Xuan, and R. P. Roberto, "Tunable silicon microring resonator with wide free spectral range," *Appl. Phys. Lett.* **89**, 071110 (2006).
15. W. M. J. Green, H. F. Hamann, L. Sekaric, M. J. Rooks, and Y. A. Vlasov, "Ultra-compact reconfigurable silicon optical devices using micron-scale localized thermal heating," in *Optical Fiber Communication and the National Fiber Optic Engineers Conference, 2007. OFC/NFOEC 2007.* (2007), pp. 1-3.
16. M. Lipson, "Compact Electro-Optic Modulators on a Silicon Chip," *Photonics in Switching*, 67-68 (2006).

17. M. W. Geis, S. J. Spector, R. C. Williamson, and T. M. Lyszczarz, "Submicrosecond submilliwatt silicon-on-insulator thermo-optic switch," *IEEE Photon. Technol. Lett.* **16**, 2514-2516 (2004).
18. G. Cocorullo, F. G. Della Corte, I. Rendina, and P. M. Sarro, "Thermo-optic effect exploitation in silicon microstructures," *Sens. Actuators A: Phys.* **71**, 19-26 (1998).
19. D. Geuzebroek, E. J. Klein, H. Kelderman, and A. Driessen, "Wavelength tuning and switching of a thermo-optic microring resonator," *Proc. ECIO*, pp. 395-398 (2003).
20. F. Xu and A. W. Poon, "Silicon cross-connect filters using microring resonator coupled multimode-interference-based waveguide crossings," *Opt. Express* **16**, 8649-8657 (2008).
21. F. Gan, T. Barwicz, M. A. Popovic, M. S. Dahlem, C. W. Holzwarth, P. T. Rakich, H. I. Smith, E. P. Ippen, and F. X. Kartner, "Maximizing the Thermo-Optic Tuning Range of Silicon Photonic Structures," in *Photonics in Switching* (2007), pp. 67-68.
22. N. Han-Yong, R. W. Michael, L. Daqun, W. Xuan, M. Jose, R. P. Roberto, and P. Kachesh, "4 x 4 wavelength-reconfigurable photonic switch based on thermally tuned silicon microring resonators," *Opt. Eng.* **47**, 044601 (2008).

1. Introduction

Photonic Networks-on-Chip (NoC) have recently become popular as a viable option for increasing the bandwidth, lowering the latency and reducing the power in chip multiprocessors (CMPs) [1-3]. By utilizing an optical network to link multiple processors the full capability of large on-chip parallel systems can be achieved [4]. However such an optical network is only practical if it is fabricated monolithically as part of the electronics, reducing the complexity of manufacturing to a few additional CMOS steps. For this reason silicon photonics is the ideal candidate for future NoCs.

A key element in any networked system is the ability to route; that is the ability to dynamically select the destination for an input source on the network. Passive routing is typically performed by routing signals based on their wavelengths [5-9]. The problem with this scheme is that it requires as many light sources as the network has distinct paths. This leads to problems in scaling due to the necessary physical space and power consumption required by each light source.

Single wavelength networks, however, typically suffer from contention problems, since multiple signals cannot overlap on the same optical wire. We look then for hitless solutions, which we define in this paper as being spatially non-blocking, such that any of the inputs can be routed to any of the available outputs without using the same physical path. In this paper we demonstrate a 4x4 hitless router for use in an electronically-integrated optical network. The router operates on a single wavelength making it more easily scalable to any size network.

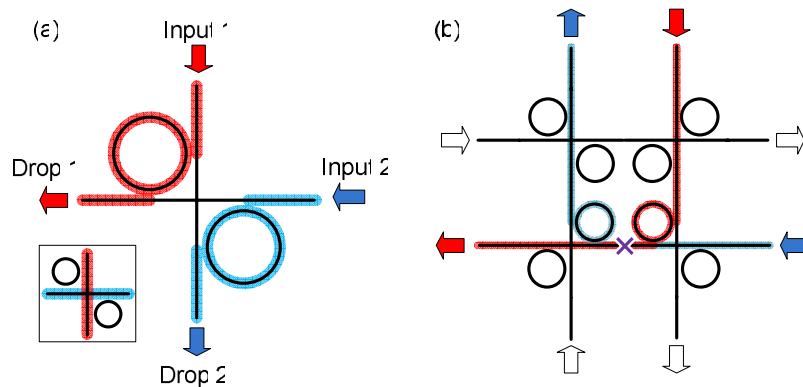


Fig. 1. Microring resonators are used as individual routing devices; (a) an active switching element switches light at an intersection (insert shows switches in off state), (b) a simple 4x4 routing device highlighting a contention state where a red and a blue signal have used the same physical path.

2. Router architecture

Switching can in principle be accomplished by adding microring resonators alongside waveguide intersections [10]. By way of selective wavelength filtering a microring resonator coupled to two waveguides can allow light to pass through, or if activated, switch the light to the intersecting waveguide. Such a switch does not take full advantage of all the available waveguides. If instead we have two rings opposite each other on a single intersection they can utilize both waveguides fully by creating the deflection switch shown in Fig. 1(a). Arranging single or double ring switches in a simple mesh configuration to create a 4x4 router has been shown before [10], but presents the obvious disadvantage of being spatially blocking (seen in Fig. 1(b)); a limiting factor in modern parallel processing devices such as CMPs.

Instead we show here a new bidirectional 4x4 configuration proposed recently by Bergman *et al* [11, 12] which allows for parallel hitless routing using the same microring resonators. Hitless routing is accomplished by having one dedicated waveguide for each input-output combination. In this topology signals are never routed to their direction of origin or to the same direction as another signal, such that there are 12 possible physical paths; 3 for each input direction as shown in Table 1(a). When these paths are operating in parallel there can be no overlap so that the number of router states (where each state specifies four paths) is reduced to 9 as seen in Table 1(b). Each of the paths uses at most one ring resonator, so that the router uses zero, two or four ring resonators to establish each of the router states.

Table 1. Router Path and State Organization

		Input				Rings Used
		N	S	E	W	
Output	N		R3	none	R1	
	S	R6		R8	none	
	E	none	R7		R5	
	W	R2	none	R4		

		I/O Combination				Rings Used
		N	S	E	W	
State Number	1	W	N	S	E	R2,R3,R8,R5
	2	W	E	N	S	R2,R7
	3	W	E	S	N	R2,R7,R8,R1
	4	S	N	W	E	R6,R3,R4,R5
	5	S	W	N	E	R6,R5
	6	S	E	W	N	R6,R7,R4,R1
	7	E	W	S	N	R8,R1
	8	E	W	N	S	none
	9	E	N	W	S	R1,R4

Four router paths establish a router state in which four connections can transfer information in parallel. (a) Each input to output combination will use one or less micro-resonators. (b) The router operates in one of nine states, each defining four paths.

In Fig. 2 the router is shown with a sample configuration of four optical non-interacting paths which are established by switching four of the rings. The multiple colors depict different signal paths, which all share the same wavelength. In the state depicted, #1 from Table 1(b), the router uses the maximum number of simultaneous rings as all channels are being switched.

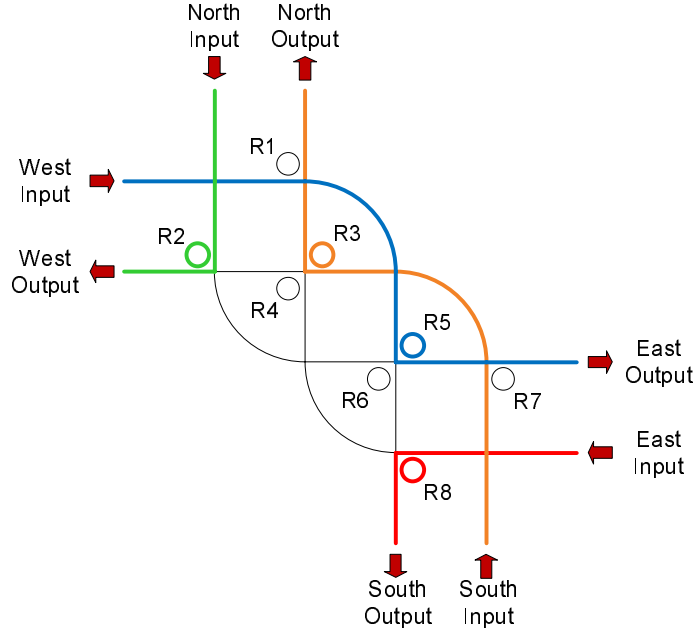


Fig. 2. The new 4x4 routing device is characterized by its multiple internal paths and ring resonator switching elements, allowing for dynamic hitless networking. Shown in color are four paths highlighting an arbitrary configuration using the maximum number of microrings.

3. Switching design

The microring resonators used in the proposed router are particularly useful since they can selectively filter a specific frequency with a device-designed amount of bandwidth, and pass it along to a different waveguide, and in so doing switch the direction of light. Specifically an input signal is “switched” when the following resonance condition is met [13]:

$$m\lambda_0 = n_{eff}L. \quad (1)$$

Here λ_0 is the resonant wavelength, m is an integer, n_{eff} is the effective index of the optical mode, and L is the length of the resonating cavity.

When the resonance condition is satisfied, light is passed to the drop port instead of the through port as seen back in Fig. 1(a). By tuning the refractive index of the silicon and hence the effective index of the mode, we can switch a single wavelength between the through port and the drop port. A shift of the effective index Δn_{eff} causes a shift of the resonant wavelength $\Delta\lambda = \lambda_0 \Delta n_{eff} / n_{eff}$ [14].

We have chosen to use the Thermo-Optic effect (TO) [15] because of its strong refractive index tuning in silicon ($\Delta n \sim 1 \times 10^{-2}$). Fabrication effects vary from ring to ring and aligning many of these to one wavelength requires a large amount of tuning flexibility. The TO effect has been shown to provide a large wavelength shift on the order of $\Delta\lambda \sim 20$ nm [16] while operating on a time scale of a few μ s using direct heating [17], suitable for circuit-switched networks. Note that the Electro-Optic effect (EO), known also as the free carrier plasma dispersion effect in silicon, has a faster switching time in this material below 100 ps and could also be used for switching in this device. However the amount of wavelength shift given by the EO effect is limited to about $\Delta\lambda \sim 2$ nm. In practice we need to shift a resonance as far as one Free Spectral Range (FSR) to adjust for fabrication misalignment of an individual ring’s resonant wavelength.

The TO effect provides a change in refractive index of silicon per degree Kelvin given by [18]:

$$\left(\frac{dn}{dT}\right)_{Si@1.5\mu m} = 1.86 \times 10^{-4} K^{-1}. \quad (2)$$

Fig. 3 shows how the temperature relates to the effective index in Silicon and in turn shifts the resonant wavelength of a ring.

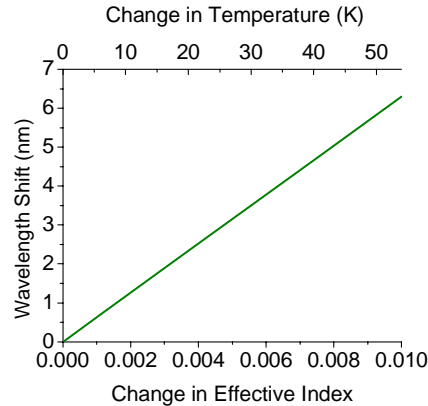


Fig. 3. The resonance wavelength shift in the microrings that is caused by the shift in effective index and equivalent temperature shift.

The configuration of the rings and heaters is determined so that the optical mode is well separated from the heater to avoid absorption while still close enough proximity to couple heat into the waveguide. We find the best arrangement of heater and waveguide using simulation. Because our heater is created from the deposition of a thin film of metal, most of the heat will be conducted from below (or above) the heater. To conduct the majority of heat we trace the heater wire above the ring resonator, creating an Ω shape, often used for microring heaters [19].

We take into consideration the size of the optical mode for our waveguide dimensions as well as the heat conduction of our heaters through the cladding material. We make our waveguides 450 nm wide by 250 nm thick, and from our finite-difference mode solver we determine that for the TE (polarized parallel to the substrate) mode, 1 μm of distance is sufficient to limit the metal absorption to $\alpha \sim 2.17 \times 10^{-4} \text{ cm}^{-1}$ (shown in Fig. 4(a)).

Confinement of heat is important due to the fact that our deflection switches have physically adjacent thermally tuned rings which would experience thermal crosstalk if the heaters were designed too wide or too close to each other. Using a 3D finite-element analysis tool we explored the most efficient way of conducting heat to our rings, while keeping the heaters small. Our final design settled on 1 μm wide wires directly above the waveguide ring in order to get a uniform, but laterally contained, heat distribution. We see in Fig. 4(b) that at 1 μm distance we can still conduct more than 56% of the temperature generated by the heater into the waveguide while still confining the heat laterally to about 5 μm from the heat source.

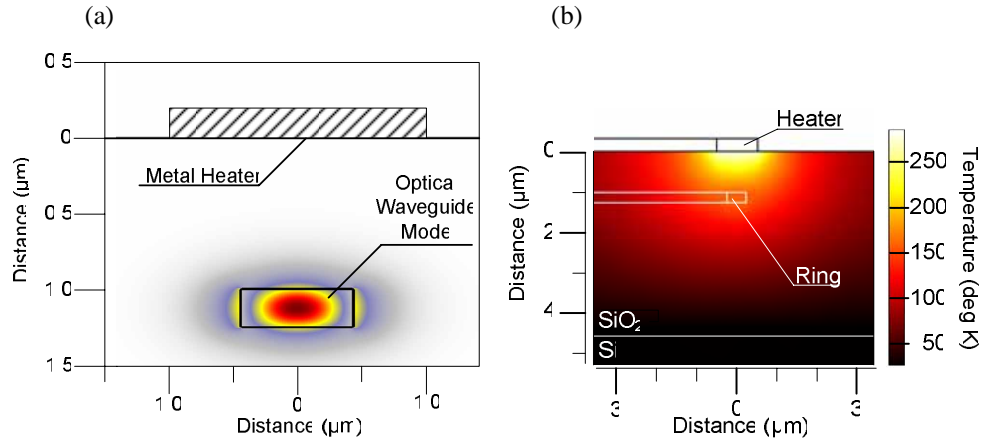


Fig. 4. Heater and waveguide design for thermal and optical efficiency: (a) the optical mode is separated from the heater to avoid absorption while (b) maintaining enough proximity to couple heat into the waveguide.

4. Device structure and fabrication

We start with commercial Silicon-on-Insulator (SOI) wafers with a 3 μm buried oxide layer. Using standard e-beam lithography we pattern the waveguides and etch them using reactive ion etching. The waveguides are then clad with 1 μm of plasma-enhanced chemical vapor deposition SiO_2 to protect the optical mode. We then planarize the top of the oxide to minimize unevenness in the following metal deposition. This step will reduce the chances of heater failure due to weak points in the metal wire.

We evaporate 300 nm of nichrome above the cladding and using a double-resist liftoff method creates the 1 μm heaters. Finally another SiO_2 cladding step protects the heaters from outside elements. The microrings use the same waveguide dimensions and have a 10 μm radius with spacing from the waveguides of 200 nm. The final system is seen in Fig. 5(a).

We also reduce the loss typically seen in waveguide intersections by transitioning adiabatically to a larger waveguide cross-section for the intersecting region. By increasing the amount of light confined within the waveguide we limit the interaction of light with the variations of the sidewalls, specifically the large scattering points created by the walls of the crossing waveguide.

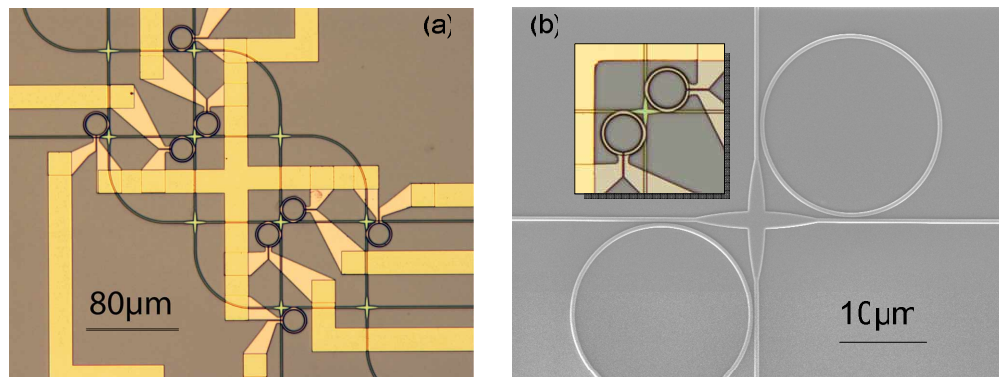


Fig. 5. Images of the fabricated router: (a) microscope image of full device shows gold contacts to nichrome heaters above the microrings; (b) an SEM image shows the details of the fabricated waveguide crossing and coupled rings (insert shows close-up of Ω heaters).

Our crossing, shown in Fig. 5(b), is simulated to have an insertion loss of -0.18 dB and better than -20 dB crosstalk to the intersecting waveguide. We have made and tested similar crossings with -0.51 dB insertion loss. MMI-based crossing designs were also considered, and could be used in future design iterations to lower the loss further [20].

5. Results

We tested the router for dynamic routing functionality. Using an Optical Spectrum Analyzer (OSA) and a broadband source, we first found all microring resonances by tuning each independently from the others. In this way we also tested the switching capabilities of the TO effect. We reproducibly tuned the ring resonances by 10 nm, which is above the FSR of these rings (8.8 nm). Switching is achieved at a rate of around 0.25 nm/mW as seen in Fig. 6, comparable to recent results for SOI microring heaters [21, 22]. An extinction ratio of 17 dB can be achieved with less than 2 mW or greater than 21 dB using 6.5 mW. We can also see that our resonances have a FWHM of 0.31 nm which corresponds to a bandwidth of around 38.5 GHz.

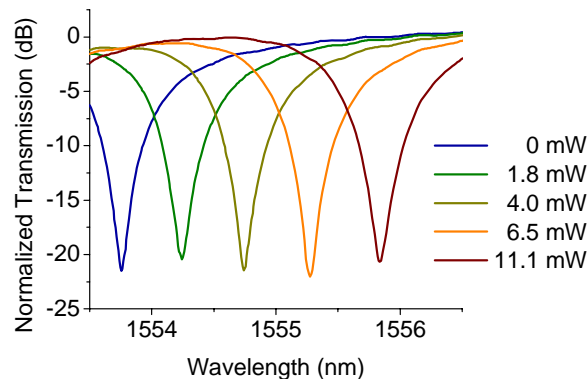


Fig. 6. Electric power applied to the heaters shifts the microring resonances, causing a switch in the transmitted optical power of a given wavelength.

We tested the router by coupling a movable tapered-lens fiber to each of the input waveguides and coupling the output from the chip to another fiber using a collimating lens. A tunable CW laser was used at 1553.67 nm in all of the tests as the input. For each input port the light was routed to all available outputs where power measurements were taken. Each of the input ports has three routing possibilities for a total of 12 unique routing paths. Because the chip was not packaged, we were physically limited from testing the third output of each input directly such that only eight of the paths were tested directly. Four paths which routed in the direction of the input facet of the chip were measured as drops of power at their respective through ports and were seen to be consistent with the results for the other eight paths.

For each of these tested paths we looked at the extinction ratio between the signal being routed to the measurement output and the remaining signal when routed away. Fig. 7 shows two of the inputs routing to one output. In Fig. 7(a) North to East is routed directly through the waveguide, and bypasses four rings along its path which are detuned from the laser frequency. It is then routed by the thermally tuned R6 microring to the south direction, which is seen at the output as a reduction of power (shown in the same graph). The two measurements shown are taken using the same input and output to compare the extinction ratio. Conversely in Fig. 7(b) we switch inputs to measure the signal being routed West to East through R5 and compare it to the same output when R5 is detuned. All other available optical paths were likewise tested showing a maximum extinction ratio of 20.79 dB for a routed signal.

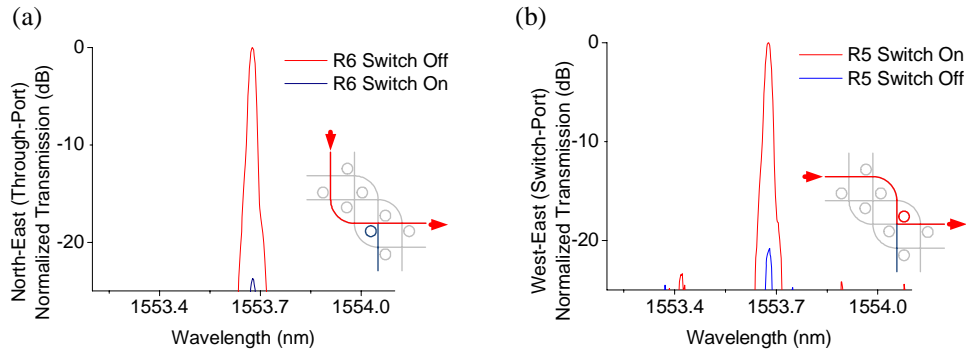


Fig. 7. Extinction ratio comparison for two switched paths: (a) the power before and after switching is measured at the through port. (b) The power before and after switching is measured at the drop port.

6. Conclusion

In summary we have fabricated and shown a working 0.07 mm^2 4×4 dynamic hitless router on SOI technology that could be used in future CMP optical networks. The device is constituted by eight $10 \text{ }\mu\text{m}$ radius microring resonators in an arrangement that provides efficient and spatially unblocking internal routing. The resonators are individually tuned by means of micro-heaters fabricated out of thin films of nichrome, which are powered by DC current to create a resonance shift. The heater/ring design has a switching power of 0.25 nm/mW . Each of the available paths is individually tested using a tunable laser and OSA for routing extinction ratio which provides a maximum of 20.79 dB and a bandwidth of 38.5 GHz . Following work will require optical packaging to establish relative power scales to compare crosstalk effects as well as relative insertion loss of the various routes in the device.